

Research Article

Wear and Friction Evaluation of Different Tool Steels for Hot Stamping

Maidier Muro,¹ Garikoitz Artola,¹ Anton Gorriño,² and Carlos Angulo² 

¹*Metallurgy Research Centre IK4 AZTERLAN, Aliendalde Auzunea 6, 48200 Durango, Spain*

²*Department of Mechanical Engineering, University of the Basque Country (UPV/EHU), Plaza Ingeniero Torres Quevedo 1, 48013 Bilbao, Spain*

Correspondence should be addressed to Carlos Angulo; carlos.angulo@ehu.es

Received 6 November 2017; Revised 12 February 2018; Accepted 22 February 2018; Published 26 March 2018

Academic Editor: Akihiko Kimura

Copyright © 2018 Maidier Muro et al. This is an open access article distributed under the Creative Commons Attribution License, which permits unrestricted use, distribution, and reproduction in any medium, provided the original work is properly cited.

The aim of this work is to investigate the durability of tool steels for hot stamping by comparing the wear resistance of three hot work tool steels. Friction and wear behaviours of different tool steels sliding against a 22MnB5 uncoated steel at elevated temperatures were investigated using a high-temperature version of the Optimol SRV reciprocating friction and wear tester at temperatures of 40 and 200°C. Our results show that friction decreased with increasing temperature, whereas wear of the tool steel increased with temperature for the second and the third tested tool steels. The slightly better wear behaviour of steel specimen 1 comes from the hardness of the carbides in the martensitic microstructure, which are rich in vanadium.

1. Introduction

Over the past several years, the automotive industry has experienced a large growth in the manufacturing of ultrahigh-strength steel (UHSS) components, especially those who can be processed by means of hot stamping technology. This increase is related to improvements obtained with these steels in terms of crash resistance and fuel consumption reduction. The benefits of employing UHSS components are accompanied by important technological challenges though, since the particularities of the transformation of these steels have nothing to do with those of conventional steels. One of the UHSS transformation related knowledge areas which is not yet well understood is the tribological interaction between the forming tools and the UHSS parts at high temperatures during the hot stamping process. In sheet metal forming, the wear of tool steels continues to be a great concern to the automotive industry because of increasing die maintenance costs and scrap rates. Cold forming tools are subjected to severe tribological stresses due to high contact pressures arising via sliding contact between the die and the sheet materials. This results in high frictional heat generation, which affects both the bulk

material and wear properties of the tool steel [1]. Since hot stamping tools are subjected to high temperatures, the wear of tool steels and the prevailing wear mechanisms have been studied in detail [2, 3]. Several authors have also studied wear behaviour in friction processes using specific tribological tests, in order to characterize different tool steel grades, with and without coatings, at elevated temperatures [3–5].

Understanding the factors that influence the wear mechanisms is necessary to minimize the rate of tool wear in hot stamping. This knowledge could be used to aid tool material selection and die design and hence increase the life of die materials used in hot stamping [6, 7].

To ameliorate the surface deterioration in hot stamping tools, it is necessary to achieve a more in-depth understanding of wear failure mechanisms [8–10]. The wear mechanisms involved in tool damage are determined by factors that are directly related to the mechanical properties of the materials. It is considered that the response to wear can be improved by means of structural martensitic changes [11].

The purpose of this article is to compare three specimen tool steels and assess which behave best against wear during

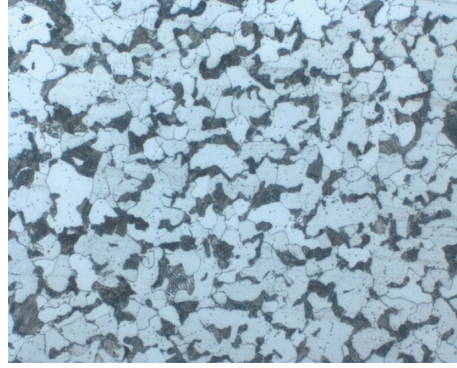


FIGURE 1: Microstructure of the pin is composed of ferrite and pearlite.

TABLE 1: Chemical composition of 22MnB5 (wt.%).

Material	C	Si	Mn	P	S	Al	Cr	B
22MnB5	0.24	0.11	0.97	0.009	0.002	0.034	0.25	0.0046

TABLE 2: Heat treatment of hot work tool steels.

Material	Hardening treatment			
	Austenitizing (°C)	Austenitizing (s)	Tempering (°C)	Tempering (s)
Steel 1	1030	1800	610–610	7200
Steel 2	1050	1800	510–510	7200
Steel 3	1040	1800	520–520	7200

TABLE 3: Chemical composition (wt.%) and hardness of hot work tool steels.

Material	Mn	Cr	Mo	V	C	Si	Hardness (HRC)	Hardness (HV)
Steel 1	0.75	2.6	2.25	0.9	0.38	0.3	51	527
Steel 2	0.25	4.5	3.0	0.55	0.50	0.2	57	632
Steel 3	0.4	6.5	1.3	0.8	0.42	0.5	56	612

press hardening. We interpret our results in the context on the microstructural features.

2. Experimental Procedure

2.1. Experimental Materials and Specimens. The study and the comparison of the wear behaviour of three tool steels were carried out with a tribopair composed of a boron steel without coating in annealed condition known as 22MnB5 (ferritic-pearlitic microstructure, Figure 1). The chemical composition of 22MnB5 is presented in Table 1.

The tool steels were tested in a hardened condition (quenched and tempered) with a tempered martensitic microstructure. The heat treatments applied to the tool steels are shown in Table 2. The austenitizing and tempering times are 30 minutes and 120 minutes, respectively. The nominal chemical composition of the tool steels (provided by material suppliers) and the final tool hardness are given in Table 3.

The tool steel specimens were flat disks ($\varnothing 24$ mm and 7.9 mm thick) and were polished to a surface Ra roughness level below 0.09 microns in order to remove any marks and reduce the number of possible influencing variables during the tests. The counter specimens were cylindrical pins ($\varnothing 2$ mm and 8 mm long) flat-end made from 22MnB5 boron steel. This geometry of the counter specimen was chosen with the objective of maintaining a constant contact pressure even if the pin specimen was subjected to high wear.

2.2. Test Equipment. The equipment used in this study was a reciprocating sliding friction and wear tester SRV model 8.110. The SRV machine, provided with an electromagnetic drive, allows the upper specimens (22MnB5 pins) to oscillate under normal load against a stationary lower test specimens (tool steel disks), as shown in Figure 2. The selected normal load was applied by a servo motor. The lower test specimen holder was provided with a heater

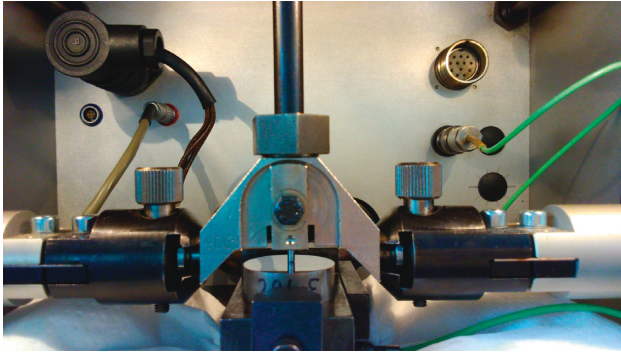


FIGURE 2: Upper and lower specimens in the SRV machine.

which permits to condition the test disks at the selected temperature. The SRV tribometer was equipped with a computerized data acquisition and control system, so that the applied load, temperature, stroke length, and frequency of the oscillatory movement were controlled and monitored.

The selection of the test parameters was based on typical hot stamping pressure used in industrial applications. The parameters were a load of 31 N, a nominal pressure of 10 MPa, a stroke length of 4 mm, temperatures of 40 and 200°C, a frequency of 25 Hz, and duration of 900 s. The total length of each test was 90 m.

2.3. Test Procedures. The tests were performed at temperatures of 40°C and 200°C. Before the tests started, all disks and pins were ultrasonically cleaned first in ether for 5 min and then for 5 more min in acetone. After that, all specimens were cleaned with paper and placed in a dryer to eliminate all possible moisture. The specimens were held in the dryer until the tests started, and before the beginning of each test, the specimens were weighted.

The tests started with the heating of the lower specimen (tool steel) to the desired temperature and held for 5 min at that set-point in order to ensure a homogenous temperature distribution along the disk. The upper pin specimen was kept separated from the disk during the heating sequence. After the disk reached the test temperature and the 5 min dwell time was over, the pin was brought into contact with the disk, the load was applied, and the test was performed.

Once the test was finalized, each specimen was cleaned again ultrasonically for 5 min in ether and 5 more min in acetone. After the cleaning, the wear of the disk and pin was measured. The measurements of the weight loss of the specimens were made with a precision weighting scale model Mettler Toledo XP205. The wear volume of the disks was also measured using a Nikon Eclipse ME600 confocal microscope.

The wear scars of the disk and the microstructure were examined with an Ultra Plus Zeiss Field Emission Gun-Scanning Electron Microscope (FEG-SEM), and the nature of the carbides in the tool steels was analysed via an Energy-dispersive X-ray Spectroscopy (EDS) analysis.

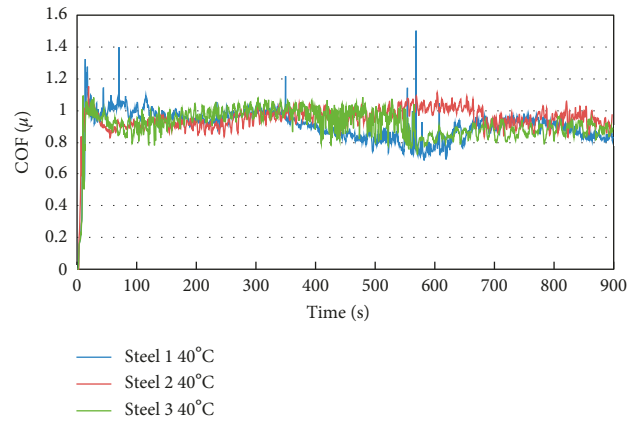


FIGURE 3: COF of the tests performed at 40°C.

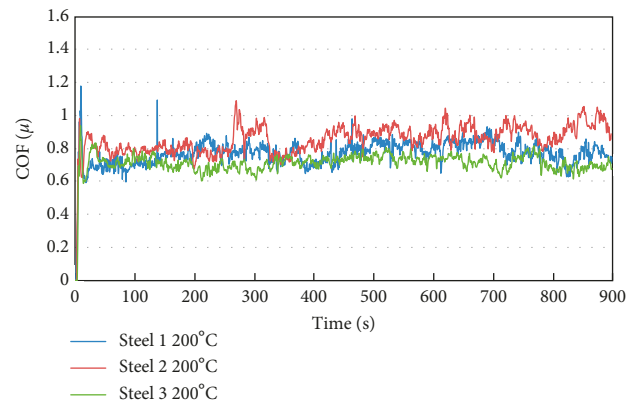


FIGURE 4: COF of the tests performed at 200°C.

TABLE 4: Average COF.

Material	Test temperature (°C)	Average COF
Steel 1	40	0.90 ± 0.005
	200	0.80 ± 0.005
Steel 2	40	1.00 ± 0.005
	200	0.90 ± 0.005
Steel 3	40	0.80 ± 0.005
	200	0.70 ± 0.005

3. Results and Discussion

3.1. Coefficient of Friction. During each test, the evolution of the coefficient of friction (COF) with time was recorded as shown in Figures 3 and 4.

The average values of the COF obtained in the tests are presented in Table 4.

When analysing the evolution of the COF with time during the test, it was observed that the three tool steels have a similar behaviour at both test temperatures, 40°C and 200°C. There is no relation between the hardness level and the COF for the three tool steels, and the COF decreases by around 15% as the test temperature increased

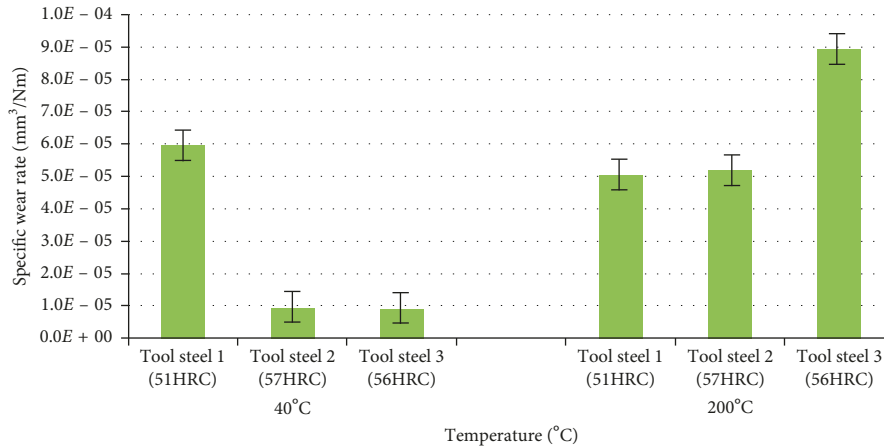


FIGURE 5: Specific wear rate of the disks at 40°C and 200°C.

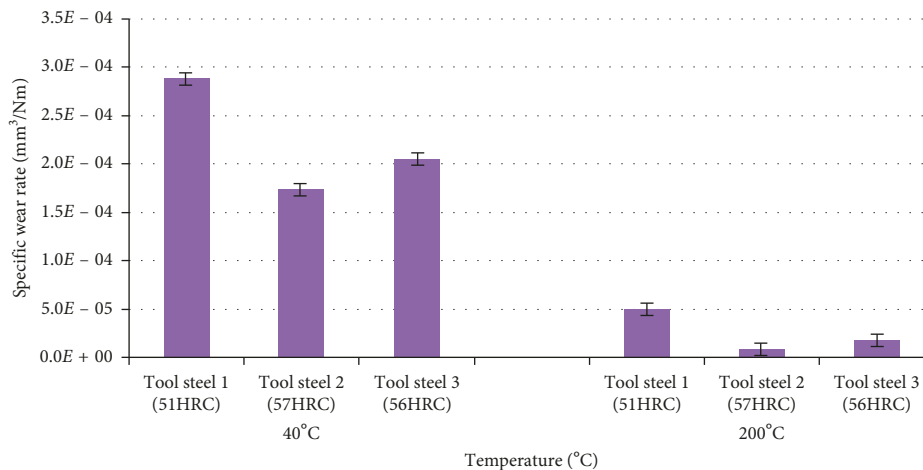


FIGURE 6: Specific wear rate of the pins at 40°C and 200°C.

to 200°C. This tendency was previously observed by others authors [3].

3.2. Wear. The evolution of the pin wear was measured in terms of specimen weight loss. For the disks, the wear characterization was made by quantifying the weight loss and the volume loss/increase with a confocal microscope. Figures 5 and 6 show the specific wear rates of the three tested group of materials (disks and pins).

3.2.1. Weight Loss. At a temperature of 40°C, the pin and disk weight losses for the tests with steel 2 and steel 3 were lower than the results obtained for steel 1. The tests with steel 3 stand out because they present the lowest wear in the disk and an intermediate wear on the pin. This behaviour is related with the hardness level of the steel 3 (56 HRC). Nevertheless, the differences in weight loss between the steel 2 and steel 3 disks were not large.

At a temperature of 200°C, the pin wear was lower than that at a temperature of 40°C. Regarding the disks, steel 1 and steel 2 present similar wear even though their hardness are different, that is, 51 HRC and 57 HRC, respectively. Steel 3 showed the highest wear despite its high hardness (56 HRC). Nevertheless, it is important to emphasise that the wear behaviour of these three steels at 200°C is similar despite their hardness differences.

A difference in behaviour, as a function of temperature, was clearly observed for the three tool steel samples. Higher differences were observed at 40°C, where steel 2 and steel 3 presented lower wear in comparison with steel 1. As the temperature increased to 200°C, oxide formation may occur, which decreases pin wear. In contrast, as the test temperature increased, disk wear increased, mainly for steel 2 and steel 3.

3.2.2. Wear Rate. In addition to the weight and volume loss, the wear rate of the pins and disks was calculated. The specific wear rate (k) is expressed by

$$k = \frac{V}{F_N \cdot s} = \frac{\Delta m / \rho}{F_N \cdot s} = \frac{\Delta m}{\rho \cdot F_N \cdot s}, \quad (1)$$

where V (mm^3) is the volume loss, Δm (kg) is the weight loss, ρ (kg/mm^3) is the density, F_N (N) is the applied normal load, and s (m) is the sliding distance. Figures 5 and 6 show the specific wear rates for the disks and pins, respectively.

Studying the results obtained from the specific wear calculation, it is concluded that the change in test temperature from 40°C to 200°C influences the tribological behaviour of the three analysed tool steels against 22MnB5, at least for steel 2 and steel 3. As mentioned by other authors [3], as the temperature increases, the COF decreases while the wear of the tool increases. In order to verify if the wear increase is related to the thermal softening (tempering) of the tool steels, the hardness of the disks tested at 200°C was checked on the wear tracks, and no variations from the initial values were found. Thus, the increase of the specific wear rate in the present work is not related with any softening, since the specimens tested at 200°C maintained their hardness after the test.

It was seen that steel 1 had similar wear rates at both 40°C and 200°C . This behaviour has been also reported by Deng et al. [6] who analysed the wear of hot work tool steel against 22MnB5 steel without coating and observed that the wear rate at 200°C was lower than that at 40°C . Similar results have been presented elsewhere [3] on studies made with 22MnB5 steel; as the test temperature increased, the wear of the disk of tool steel decreased. This behaviour is understood to be related to the formation of a compact oxide layer which protects the surface from wear.

It is worth remarking that, although the wear response of steel 1 was the poorest at 40°C , the three studied steels behaved nearly the same at 200°C . This effect of equalization at high temperature has also been reported for tool steels [2]. Regarding the wear rate of the pins, all specimens tested at 40°C showed a much higher rate than the tool steels.

By analysing the surface of the disks with electron microscopy (FEG-SEM/EDS), the disks of steel 2 and steel 3 show debris from an oxide layer on the surface, which is related with the low wear rate. The layer protects the disk surface against wear (Figures 7–10), which avoids metal-metal contact. The noncompacted wear debris particles caused an abrasive wear on the disk surfaces.

3.3. Contact Path. After each test, the profile disk of the contact paths was characterised by measuring the maximum profile height and depth as shown in Figures 11–13, where the vertical axis shows the height (z) and the horizontal axis shows the width (x).

By analysing the contact path, the shallowest groove depths were measured for steel 2 and steel 3 at 40°C , with values of 7 and $10\ \mu\text{m}$, respectively (Figures 11 and 12). Additionally, from contact profilometry measurements, it was verified that the profile height increases due to the presence of an oxide layer in some zones on the surface.

In contrast, steel 1 showed a larger amount of wear. In this case, the disk surface presented numerous grooves,

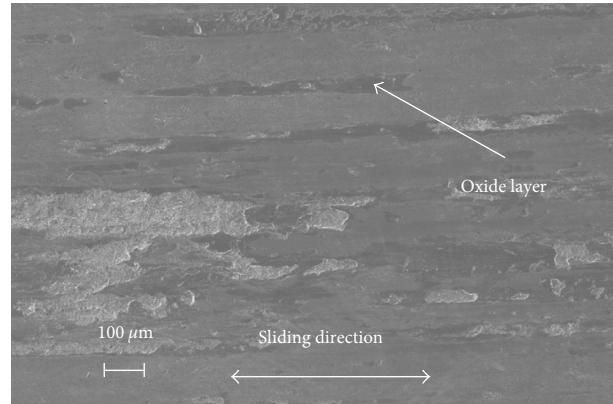


FIGURE 7: Scanning electron microscope micrograph of the steel 2 disk surface tested at 40°C .

and zones covered by a compact oxide layer were hardly identified (Figure 14). The maximum groove depth reached $25\ \mu\text{m}$ (Figure 13).

It is concluded that at 40°C test temperature, the harder the tool steel is, the higher the abrasive wear resistance, which explains the lower values of wear rate obtained for steel 2 and steel 3. In this case, the wear resistance is governed by the hardness of the martensitic matrix. Hence, the lower hardness of the steel 1 disk is not enough for it to withstand the large abrasive action occurring between the disk and the pin, which leads to a high groove formation and consequently high abrasive wear.

At a 200°C test temperature, the surface characteristics and the wear rates of three tool steels were very similar. Despite the large hardness of tool steels, a lower wear rate value is related to the presence of an oxide layer that partially covers the disk surface, thus protecting it against wear. It is assumed that the formation of the oxide layer is similar for the three tool steels. The surfaces were characterized by electron microscopy (Figures 15 and 16) and via contact profile measurements (Figures 17–19). It was observed that the wear of the three steel disks was abrasive, with maximum depths of the grooves between 29 and $38\ \mu\text{m}$.

In relation with the wear rate of the disks at the 200°C test temperature, the results are similar with those presented by other authors [3, 6], and the differences between results were probably caused by the different roughness of the specimens. In these works, the authors observed an agglomeration and compacting of oxidized wear debris in the tool steel surface that formed a protective layer against wear. This layer was able to stand the load and avoid the metal-metal contact during the test.

In this work, some zones with a protective oxide layer were also observed. In the case of steels 2 and 3, the wear rate increased by one order of magnitude from the test performed at 40°C to the test at 200°C (Figures 5 and 6). In the case of steel 1, an increase in the test temperature presented a slight decrease in the wear rate.

Regarding the analysis of the three steel surfaces tested at 200°C , an accumulation of wear debris due to the abrasive action suffered by the disks (Figures 15 and 16)

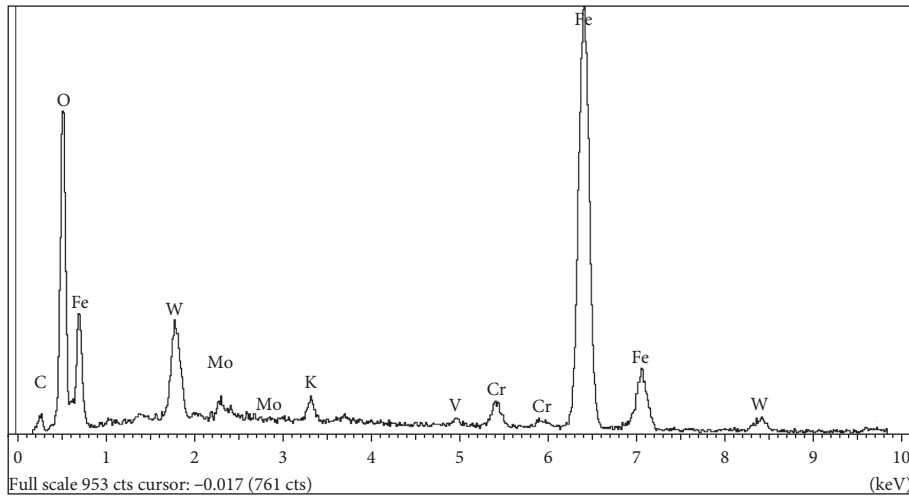


FIGURE 8: EDS spectrum of the oxides in Figure 7.

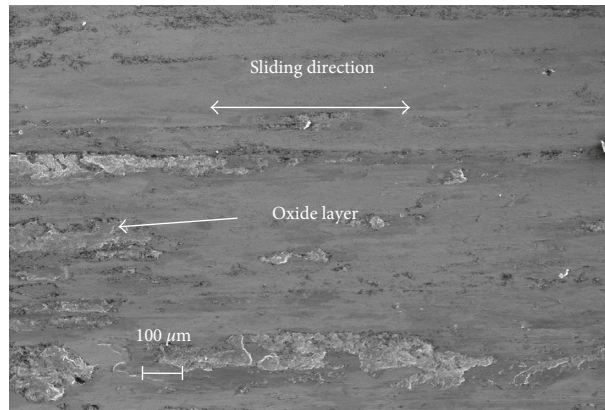


FIGURE 9: Scanning electron microscope micrograph of the steel 3 disk surface tested at 40°C.

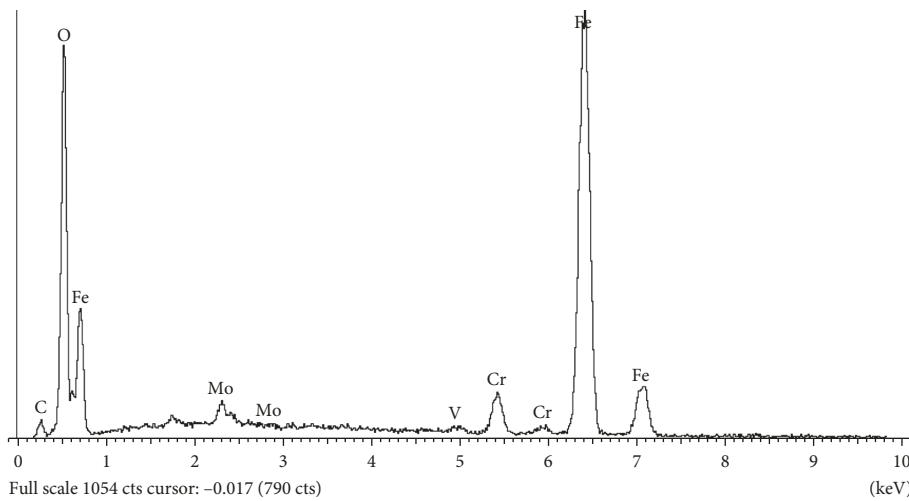


FIGURE 10: EDS spectrum of the oxides in Figure 9.

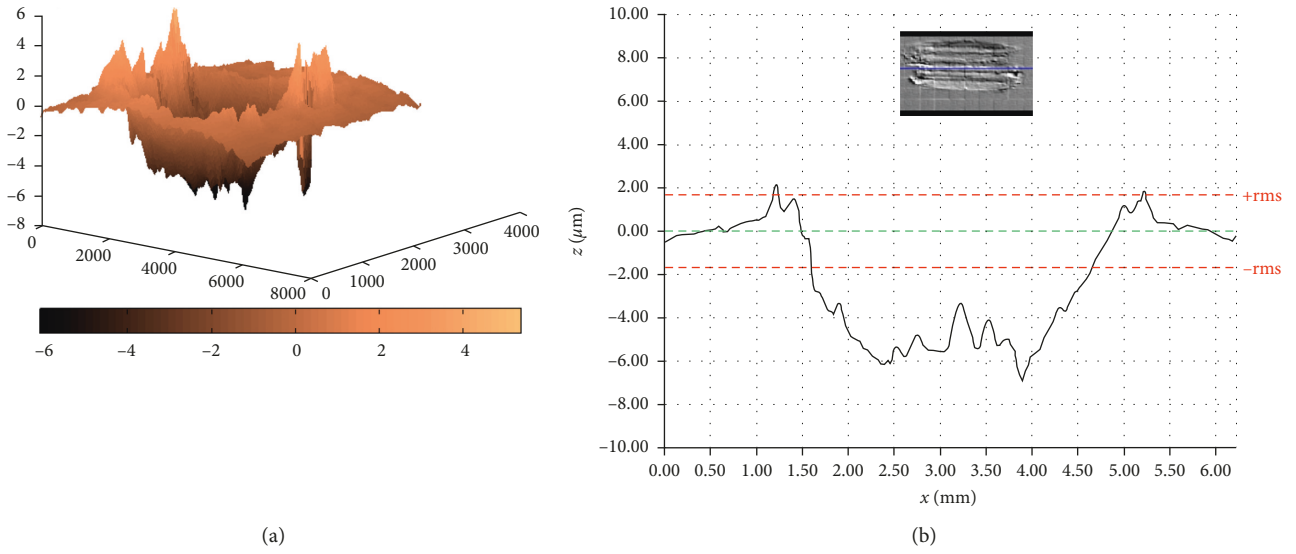


FIGURE 11: Three-dimensional image of the disk track of steel 2 tested at 40°C (a). The maximum profile depth (7 μm) (b).

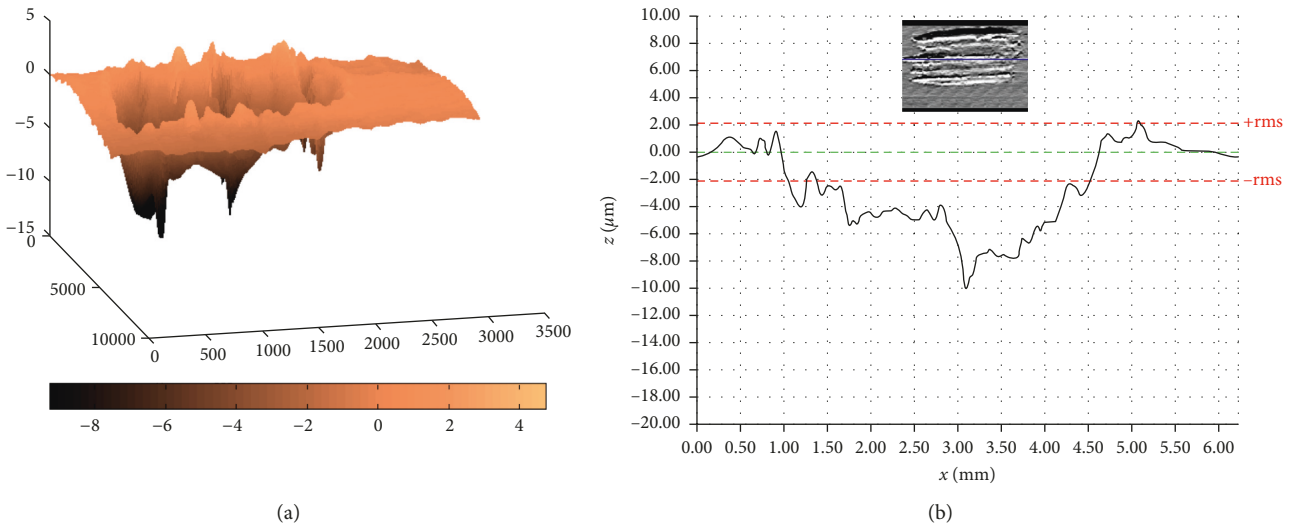


FIGURE 12: Three-dimensional image of the disk track of steel 3 tested at 40°C (a). The maximum profile depth (10 μm) (b).

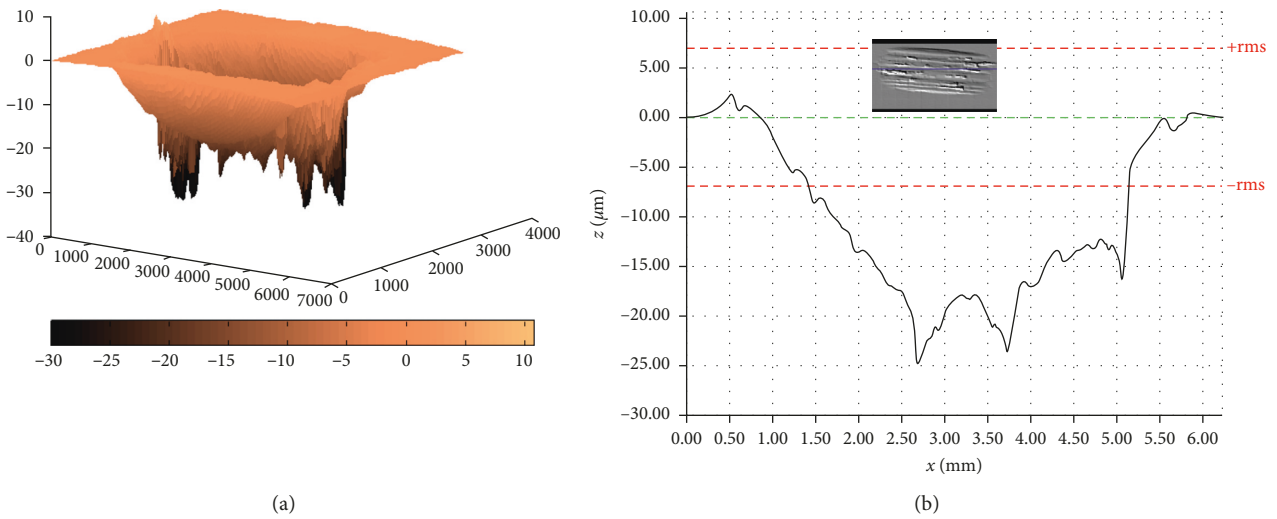


FIGURE 13: Three-dimensional image of the disk track of steel 1 tested at 40°C (a). The maximum profile depth (25 μm) (b).

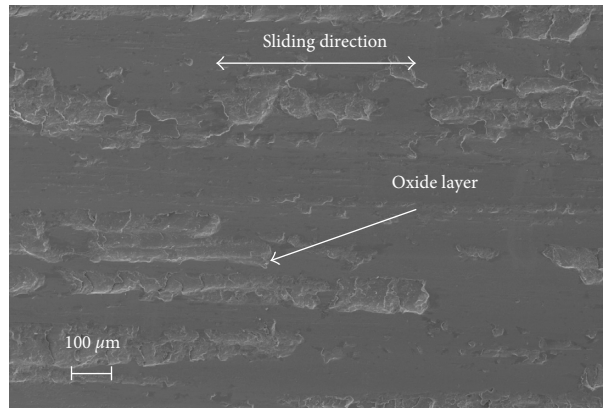


FIGURE 14: Scanning electron microscope micrograph of the steel 1 disk surface tested at 40°C.

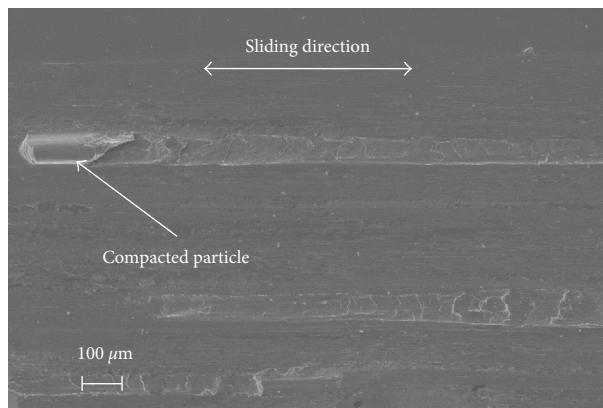


FIGURE 15: Scanning electron microscope micrograph of the steel 1 disk surface tested at 200°C.

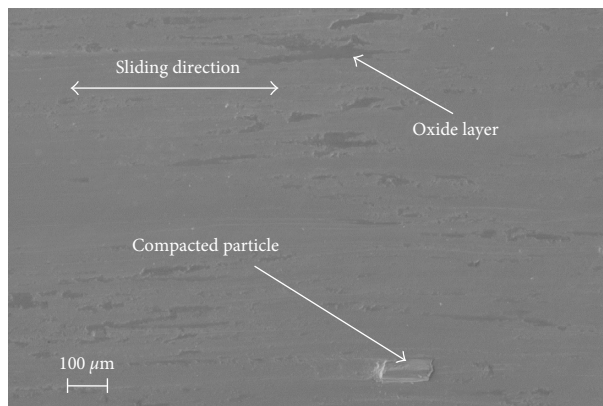


FIGURE 16: Scanning electron microscope micrograph of the steel 2 disk surface tested at 200°C.

was observed. Despite the wear debris accumulation, some zones of the surface were covered by an oxide layer (Figure 16). It seems that the release of the oxide layer particles causes a three-body wear that causes large abrasive wear in the disk surface and generates deep depth grooves.

When the test temperature increased from 40°C to 200°C, a high amount of oxide was observed on the disk surface, according to works in the literature [3, 6] the oxide layer should break into pieces easily below 300°C. The presence and release of oxides imply an increase in wear rate as the temperature increased. A larger amount of hard oxides

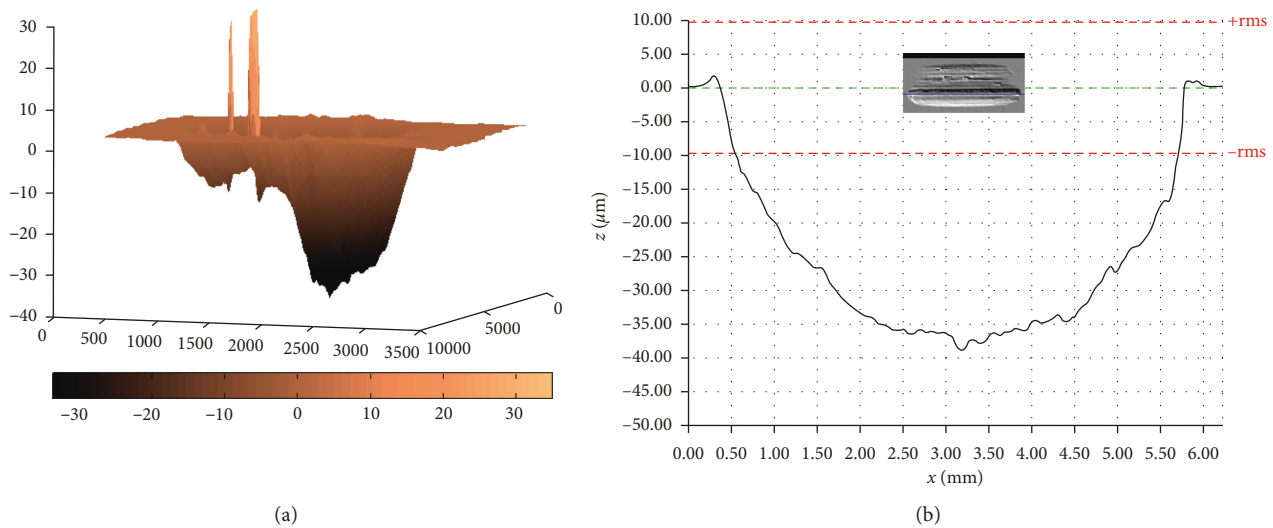


FIGURE 17: Three-dimensional image of the disk track of steel 1 tested at 200°C (a). The maximum profile depth (38 μm) (b).

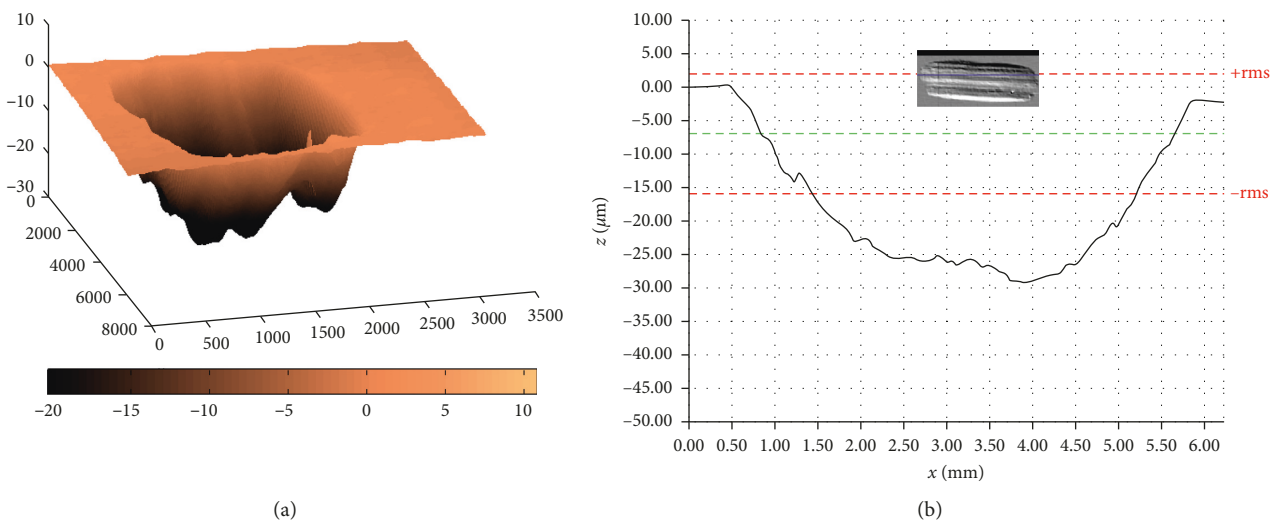


FIGURE 18: Three-dimensional image of the disk track of steel 2 tested at 200°C (a). The maximum profile depth (29 μm) (b).

directly affects the wear resistance of the tool steel when working against uncoated 22MnB5.

From the obtained results, it is concluded that at a test-temperature of 200°C, the release of oxide particles negatively affects the wear resistance of the tool steels. Also, the large hardness of tool steel 2 (57 HRC) was not enough for it to withstand the abrasive action of the oxide particles. Tool steel 1 presented the best wear behaviour, even though it had the smallest relative hardness. Analysing the chemical composition of the steels, steel 1 presented the largest vanadium content. Using a scanning electron microscope (SEM model Phillips), our EDS analysis identified the nature of the carbides in each steel sample. The carbides present in steel 2 were rich in molybdenum and the ones in steel 3 were rich in chromium. Hence, the better wear behaviour of steel 1 at 200°C is related with the nature of the carbides, which were rich in vanadium (Figure 20). In the test at 200°C, it seems that

the wear behaviour of each steel was governed by the carbide hardness present in the steel sample, rather than the martensitic matrix hardness (Figure 21).

When analysing the three carbides, the vanadium carbides, due to their hardness and chemical nature, were the most efficient at improving the wear resistance. In contrast, the chromium carbides were the less efficient (Table 5).

4. Conclusions

The results obtained from pin-on-disk tests, using a SRV tribometer and temperatures of 40°C and 200°C, were presented as a method for determining the wear behaviour and the durability of the three selected hot work tool steels.

The slight decrease observed in the COF, as the temperatures increased to 200°C, was related to oxide layer formation. Despite the drop in the friction coefficient, the

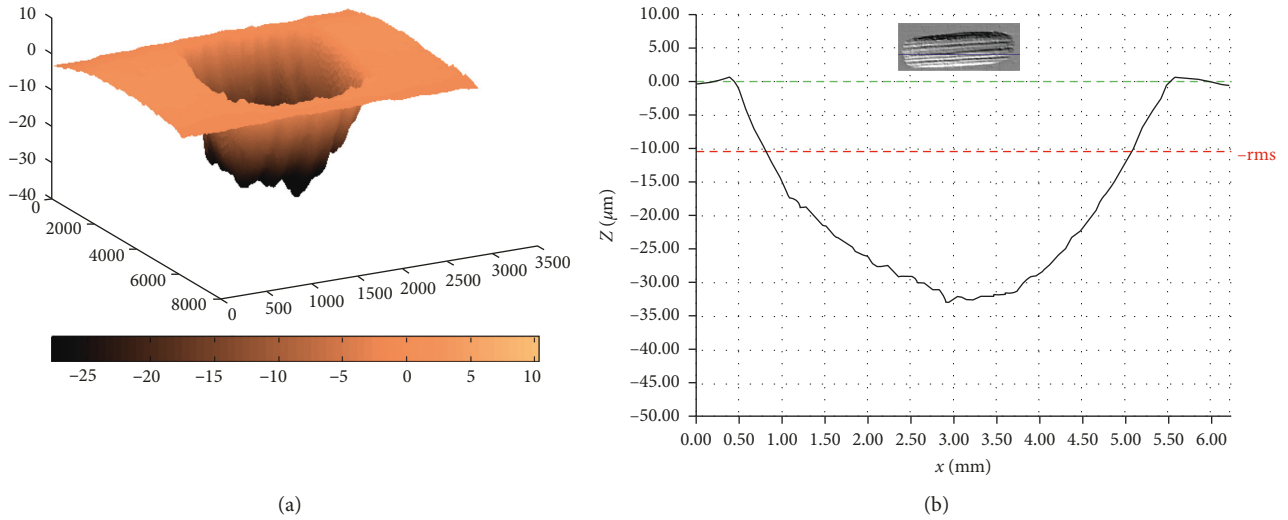


FIGURE 19: Three-dimensional image of the disk track of steel 3 tested at 200°C (a). The maximum profile depth (32 μm) (b).

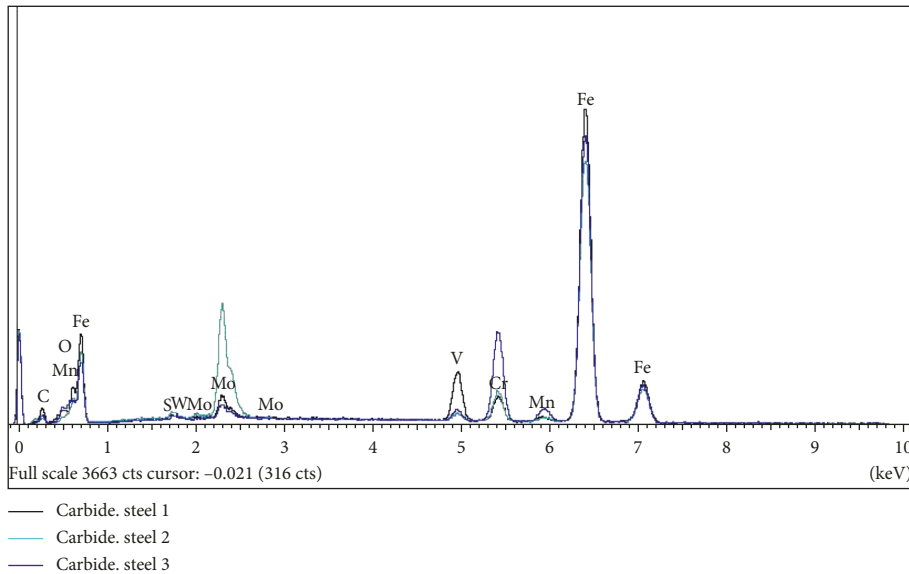


FIGURE 20: Comparison of the carbides' nature of the tool steels studied.

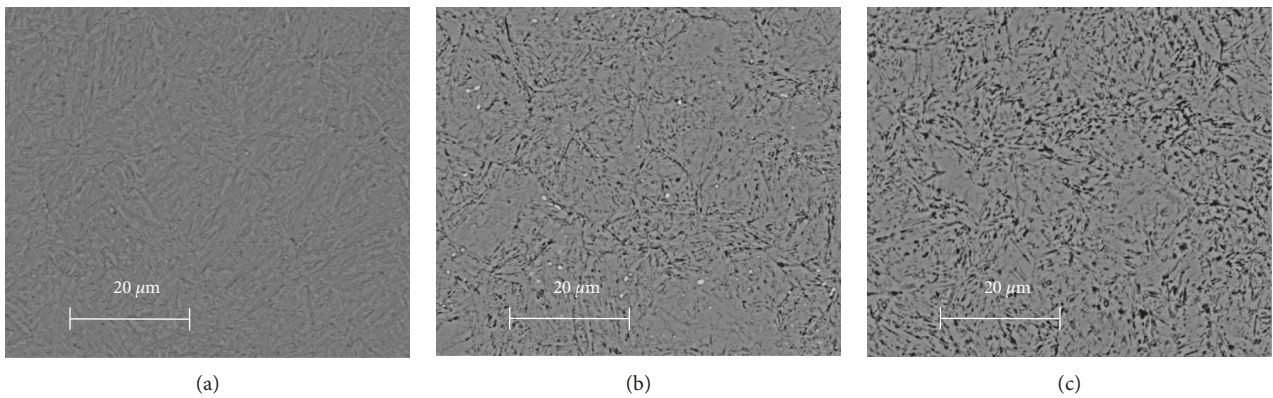


FIGURE 21: Detailed micrograph of steel 1 (a), steel 2 (b), and steel 3 (c).

TABLE 5: Different carbides hardness.

Nature of the carbide	Hardness (GPa)
Chromium carbides	10.2–20 [12]
Molybdenum carbides	13.39–28.87 [13]
Vanadium carbides	11.7–31.5 [14]

wear rate of the disks at 200°C was higher than that at 40°C for the steel 2 and steel 3 samples. At this temperature, steel 1 and steel 2 showed similar behaviour, while steel 3 performed worse.

SEM inspections confirmed that oxide layer debris, which is unstable at temperatures less than 300°C, is released from the steel surface during the SRV test. These released oxides are hard abrasive particles, leading to severe three-body wear and the formation of depth grooves. This wear mechanism affected each tool steel with different levels of severity, depending on the nature of the carbides in their microstructure. Steel 1 and steel 2, bearing vanadium and molybdenum carbides whose hardness is larger than those of the chromium carbides in steel 3, had greater wear resistance at 200°C.

It must be remarked that even though steel 1 outperformed steel 3 in terms of wear resistance at 200°C, it shows lower room temperature hardness. Thus the HRC hardness, which represents an average hardness of the martensitic matrix and the carbides of the tool steel, cannot be the only guidance when designing hot forming tool steels.

Conflicts of Interest

The authors declare that they have no conflicts of interest.

Acknowledgments

The authors gratefully acknowledge the funding provided by the Department of Research and Universities of the Basque Government under Grant no. IT947-16 and the University of the Basque Country UPV/EHU under Program no. UFI 11/29.

References

- [1] Ö. N. Cora, K. Namiki, and M. Koc, “Wear performance assessment of alternative stamping die materials utilizing a novel test system,” *Wear*, vol. 267, no. 5–8, pp. 1123–1129, 2009.
- [2] J. Hardell and B. Prakash, “High-temperature friction and wear behaviour of different tool steels during sliding against Al-Si-coated high-strength steel,” *Tribology International*, vol. 41, no. 7, pp. 663–671, 2008.
- [3] J. Hardell, S. Hernandez, S. Mozgovoy, L. Pelcastre, C. Courbon, and B. Prakash, “Effect of oxide layers and near surface transformations on friction and wear during tool steel and boron steel interaction at high temperatures,” *Wear*, vol. 330–331, pp. 223–229, 2015.
- [4] C. Boher, S. Le Roux, L. Penazzi, and C. Dessain, “Experimental investigation of the tribological behavior and wear mechanisms of tool steel grades in hot stamping of a high-strength boron steel,” *Wear*, vol. 294–295, pp. 286–295, 2012.
- [5] A. Ghiotti, F. Sgarabotto, and S. Bruschi, “A novel approach to wear testing in hot stamping of high strength boron steel sheets,” *Wear*, vol. 302, no. 1–2, pp. 1319–1326, 2013.
- [6] L. Deng, S. Mozgovoy, J. Hardell, B. Prakash, and M. Oldenburg, “Press-hardening thermo-mechanical conditions in the contact between blank and tool,” in *Proceedings of 4th International Conference on Hot Sheet Metal Forming of High-Performance Steel (CHS2)*, pp. 293–300, Luleå, Sweden, June 2013.
- [7] A. Ghiotti, S. Bruschi, and F. Borsetto, “Tribological characteristics of high strength steel sheets under hot stamping conditions,” *Journal of Materials Processing Technology*, vol. 211, no. 11, pp. 1694–1700, 2011.
- [8] G. A. Fontalvo and C. Mitterer, “The effect of oxide-forming alloying elements on the high temperature wear of a hot work steel,” *Wear*, vol. 258, no. 10, pp. 1491–1499, 2005.
- [9] L. Pelcastre, J. Hardell, and B. Prakash, “Galling mechanisms during interaction of tool steel and Al-Si coated ultra-high strength steel at elevated temperature,” *Tribology International*, vol. 67, pp. 263–271, 2013.
- [10] K. Dohda, C. Boher, F. Rezai-Aria, and N. Mahayotsanun, “Tribology in metal forming at elevated temperatures,” *Friction*, vol. 3, no. 1, pp. 1–27, 2015.
- [11] G. A. Fontalvo, R. Humer, C. Mitterer, K. Sammt, and I. Schemmel, “Microstructural aspects determining the adhesive wear of tool steels,” *Wear*, vol. 260, no. 9–10, pp. 1028–1034, 2006.
- [12] I. Hussainova, E. Hamed, and I. Jasiuk, “Nanoindentation testing and modeling of chromium-carbide-based composites,” *Mechanics of Composite Materials*, vol. 46, no. 6, pp. 667–678, 2011.
- [13] Y. Z. Liu, Y. H. Jiang, J. Feng, and R. Zhou, “Elasticity, electronic properties and hardness of MoC investigated by first principles calculations,” *Physica B: Condensed Matter*, vol. 419, pp. 45–50, 2013.
- [14] L. Wu, T. Yao, Y. Wang, J. Zhang, F. Xiao, and B. Liao, “Understanding the mechanical properties of vanadium carbides: nano-indentation measurement and first-principles calculations,” *Journal of Alloys and Compounds*, vol. 548, pp. 60–64, 2013.



Hindawi
Submit your manuscripts at
www.hindawi.com

